

Network Reconstruction Problem for an Epidemic Reaction-Diffusion

Louis-Brahim Beaufort, Pierre-Yves Massé,
Antonin Reboulet and Laurent Oudre

2021

Abstract

We study the network reconstruction problem for an epidemic reaction-diffusion. These models are an extension of deterministic, compartmental models to a graph setting, where the reactions within the nodes are coupled by a diffusion. We study the influence of the diffusion rate, and the network topology, on the reconstruction and prediction problems, both from a theoretical and experimental standpoint. Results first show that for almost every network, the reconstruction problem is identifiable. Then, we show that the faster the diffusion, the harder the reconstruction, but that increasing the sampling rate may help in this respect. Second, we demonstrate that it is possible to classify symmetrical networks generating the same trajectories, and that the prediction problem can still be solved satisfyingly, even when the network topology makes exact reconstruction difficult.

1 Introduction

Network reconstruction problems, in which one aims at reconstructing a network structure from the observation of a signal evolving on it, is an important topic of current research, spanning over numerous domains (Marc Timme and Casadiego 2014; Shandilya and Marc Timme 2011; Dong et al. 2015; Le Bars et al. 2019; Sardellitti, Barbarossa, and Lorenzo 2019). Indeed, the widespread use of networks as a modelling tool in fields as diverse as telecommunications (Pastor-Satorras and Vespignani 2004; Newman, Watts, and Strogatz 2002), genetics (Gardner et al. 2003; Karlebach and Shamir 2008), ecology (Hanski and Gilpin 1997; Tamburello, O. Ma, and M. Côté 2019), or transportation of goods or humans (Youn, Gastner, and Jeong 2008; Perfido et al. 2017), to name but a few, makes understanding the connections between their structure, or internal properties, and the phenomena which happen over them, a crucial issue.

Recently, Prasse and Piet Van Mieghem (2020) have addressed the reconstruction problem for a wide class of epidemiological models (Sahneh, C. Scoglio, and P. Van Mieghem 2013). These models have gained considerable attention since the early 20th century, following notably the classic works of Kermack and McKendrick (1927). In those, individuals are categorized in compartments which describe their status with respect to an infectious disease, and the models describe the way they transition from compartments to compartments as the disease spreads through contacts, and they react (heal) to it (Odo Diekmann, H. Heesterbeek, and Britton 2012). Quickly, the early scalar models have been enhanced, by embedding them into networks (Pastor-Satorras and Vespignani 2001; Pastor-Satorra et al. 2015; Nowzari, Preciado, and Pappas 2016), in order to refine the analysis of the influence of contacts between individuals, on the spread of the disease.

In their work, Prasse and Piet Van Mieghem (2020) ask two questions: first, can the network structure be retrieved from the observation of the dynamics? Secondly,

even in the case of a negative answer, is it possible to approximate the structure well enough to predict the future evolution of the disease? Even if the problem they study has a linear structure, they show the answers to these questions are not straightforward. We propose to address the same questions on another very important class of network-epidemiological models, the epidemic reaction-diffusion models, also known as metapopulation models with explicit movement (Arino 2009). Just like the model studied in Prasse and Piet Van Mieghem (2020), the nodes of the graph represent sub-populations: for instance, the cities in the transportation network of a country. However, the interactions between populations is no longer described by a static contact structure, but by a diffusion. Accordingly, the internal dynamics of each sub-population follow a standard deterministic epidemiological model (SIS, SEIR, ...) (Odo Diekmann, H. Heesterbeek, and Britton 2012) while flows of individuals go from node to node through a diffusion. Following their apparition in population dynamics in the 1970’s, these models have since gained considerable attention in the field of mathematical epidemiology (Brauer and Driessche 2001; Van den Driessche and Watmough 2002; W. Wang and Zhao 2005; Allen et al. 2007; Tien et al. 2015; Arino 2017). However, we are not aware the inverse problem has been studied for these models, up to now.

The standard network reconstruction procedure (Marc Timme and Casadiego 2014) is the optimisation of some regression error. However, lack of identifiability, and bad conditioning, may prevent it from being highly efficient. Structural and qualitative analysis of the model is therefore of much importance to better understand the dynamics at hand, and guide the reconstruction work. Moreover, such analysis may provide insights for other models incorporating diffusion as well (Haehne et al. 2019). Our contributions are therefore the following. On the one hand, we conduct theoretical analysis on the influence of the diffusion rate on the reconstruction, and illustrate our results by experiments. On the other hand, we study the influence of network topology, both theoretically, using notably the notion of graph automorphisms (Simon, Taylor, and Kiss 2011; Ward and López-García 2019), and experimentally. Similar questions have been asked for other epidemic models (Ganesh, Massoulié, and Towsley 2005; Durrett 2010; Vajdi and Caterina Scoglio 2018; Prasse, Devriendt, and Piet Van Mieghem 2021).

We first present background material in Section 2. Next, we present the problem we address, conduct some initial identifiability analysis, and describe the experimental setup, in Section 3. Then, in Section 4, we study the influence of the diffusion rate. Finally, in Section 5, we study the influence of the network topology. The proofs are deferred to the appendices. The code for the experiments, implemented in Python, is available on the git repository: https://reine.cmla.ens-cachan.fr/masse/network_reconstruction_reaction_diffusion.

2 Background

We first present the classical epidemiological models (Section 2.1), before giving a short overview on network reconstruction techniques (Section 2.2). Then, we present our contributions (Section 2.3). Finally, we introduce our notations (Section 2.4).

2.1 Deterministic, Compartmental Epidemiological Models

Deterministic, compartmental epidemiological models represent the propagation of a disease within a population by first segmenting the population in compartments, describing the status with respect to the disease (Odo Diekmann, H. Heesterbeek, and Britton 2012). Classical compartments include the “susceptible” (S), which gathers people which may contract the disease when confronted to “infected” (I) people, who later will have “recovered” (R). Transitions from compartments to com-

partments are governed by differential equations. One simple and generic model, which we use for simplicity throughout our study, is the SIR model. Three scalar functions s , i and r track the numbers of people in each compartment, and they evolve according to, for all $t \geq 0$,

$$\begin{cases} \frac{ds}{dt} = -\beta si \\ \frac{di}{dt} = \beta si - \delta i \\ \frac{dr}{dt} = \delta i. \end{cases} \quad (1)$$

Here, β and δ are positive real numbers. The parameter β is often called the infection rate, and δ is the curing rate. The quantity δ^{-1} may be interpreted as the average time an individual remains infected, before healing (O. Diekmann, J. A. P. Heesterbeek, and Roberts 2009). The fact it is positive means people heal in finite time. It is well-known that the system of Equation (1) has a global solution for every initial condition (s_0, i_0, r_0) with only nonnegative coordinates, and that solutions tend to equilibria of the form $(s_\infty, 0, r_\infty)$ (Odo Diekmann, H. Heesterbeek, and Britton 2012).

Works have extended these models to graphs, in order to increase their representative power (Nowzari, Preciado, and Pappas 2016). Nodes of the graphs represent either individuals, or sub-populations (cities, or countries, for instance). Accordingly, let us consider a possibly directed, (strongly, if directed) connected graph of size $N = |\mathcal{N}|$, where \mathcal{N} is the set of nodes n . In each node of the graph, a standard SIR reaction happens. We write therefore β_n the infection rate, and δ_n the curing rate, of node n . Depending on the context, we write $\boldsymbol{\beta}$ (resp. $\boldsymbol{\delta}$) the diagonal matrix of coefficients β_n (resp. δ_n), or the vector $(\beta_1, \dots, \beta_N)$ (resp. $(\delta_1, \dots, \delta_N)$). Finally, we refer to the β_n 's and δ_n 's as epidemiological parameters. As we said in the introduction, we consider the model where the internal node dynamics are coupled by a diffusion (Brauer and Driessche 2001; Van den Driessche and Watmough 2002; W. Wang and Zhao 2005; Allen et al. 2007; Tien et al. 2015; Arino 2017). It is governed by a diffusion matrix¹, which we define as follows.

Definition 1 (Diffusion Matrix). *A diffusion matrix M is first Metzler, that is for $i \neq j$, we have $M_{ij} \geq 0$. Then, it is irreducible². Thirdly, its columns have vanishing sums.*

The resulting reaction-diffusion dynamics is given by

$$\begin{cases} \frac{dS}{dt} = -\boldsymbol{\beta}S \odot I + MS \\ \frac{dI}{dt} = \boldsymbol{\beta}S \odot I - \boldsymbol{\delta}I + MI \\ \frac{dR}{dt} = \boldsymbol{\delta}I + MR, \end{cases} \quad (2)$$

where, as we explain below in Section 2.4, \odot represents the coordinate-wise product³. Standard results guarantee that the solution to Equation (2) is global, and converges to a fix point of the form $(S, 0, R)$, as $t \rightarrow \infty$ (Arino 2009). Moreover, the total population is preserved, that is $\sum_n S_n(t) + I_n(t) + R_n(t)$ is constant. Finally, standard Perron-Frobenius theory (Meyer 2000) shows a diffusion matrix admits a unique stationary distribution, that is a positive vector $\tilde{\mu}_M$ summing to

¹We adopt this terminology, for lack of a universally agreed term for these matrices.

²This is possible if the graph is directed because we ask it is then strongly connected.

³For instance, for a node n , the equation on S_n reads: $dS_n/dt = -\beta_n S_n(t)I_n(t) + \sum_{i=1}^N M_{n,i}S_i(t)$. Our notation is not standard, but we think it makes clearer the link of the graph system of Equation (2) with the scalar system of Equation (1).

1 such that $M\tilde{\mu}_M = 0$. Moreover, solutions of $dX/dt = MX$ with initial condition X_0 having a nonzero coordinate along $\tilde{\mu}_M$ converge to $\tilde{\mu}_M$, as $t \rightarrow \infty$. In particular, since the total population $S + I + R$ satisfies this equation, and its initial condition has a nonzero coordinate along $\tilde{\mu}_M$ (one quickly checks it equals $\sum_n S_n(0) + I_n(0) + R_n(0)$, which is nonzero as $S(0)$, $I(0)$ and $R(0)$ have nonnegative coordinates), it converges to this stationary distribution, as $t \rightarrow \infty$.

2.2 Background on Issues in Network Reconstruction

The network reconstruction problem from observations, where one aims at expliciting the topology of a network of N nodes, by observing the values taken by some dynamical system which evolves on it, has been extensively studied in the literature (see for instance the review (Marc Timme and Casadiego 2014)). The network is described by some matrix M (typically, the adjacency matrix, possibly weighted). Observations are often gathered in two matrices, \hat{Y} and \hat{O} , which typically belong to $\mathcal{M}_{N \times K}(\mathbb{R})$, where K is the number of measurements. Often, \hat{Y} gathers estimates of the time derivatives of the state of the dynamical system in each node, at the different measurement times, and \hat{O} is the so-called observation matrix gathering the values in each node, at the same times. Then, one knows the relation $\hat{Y} = M\hat{O}$ must be satisfied. Therefore, the problem amounts to solving this regression equation. We first describe the different observations possible, then address the solving of the regression.

Observations may first consist in measurements of the answer the system gives to some user-driven perturbation of its dynamics (Gardner et al. 2003; Yeung, Tegnér, and Collins 2002; Yu and Parlitz 2010). In the case of non linear dynamics, these perturbations may occur near a fixed point, the interest being that the first-order expansion of this system then depends linearly on the network (Gardner et al. 2003), so that the observations \hat{Y} , \hat{O} , and the network matrix M , indeed satisfy the $\hat{Y} = M\hat{O}$ equation. Alternatively, observations may be obtained through mere observation of the system (Shandilya and Marc Timme 2011; Makarov, Panetsos, and Feo 2005). The nature of \hat{Y} and \hat{O} moreover depends on whether a model for the dynamics studied is known (Shandilya and Marc Timme 2011; Gardner et al. 2003; W.-X. Wang et al. 2011; Prasse and Piet Van Mieghem 2020), or not (Quinn et al. 2011; Barzel and Barabási 2013; Mangan et al. 2016; Casadiego et al. 2017). For instance, in Bussel, Kriener, and M. Timme (2011), the authors use detailed knowledge of the evolution of a synthetic model of a biological synaptic network between spiking times, to obtain the matrices \hat{Y} and \hat{O} verifying the $\hat{Y} = M\hat{O}$ equation. On the other hand, (Casadiego et al. 2017) only assume some very general relation between the first order derivatives of the dynamical system, and the values it takes, in order to obtain similar relations.

Once obtained the observations such that the equation $\hat{Y} = M\hat{O}$ holds, one must then solve the regression problem. It may be over-determined, if $K > N$, or under determined, if $K < N$ (Stoer and Burlisch 1993). Even if X has rank N , it may be ill-conditioned, thus preventing efficient solving by mere matrix inversion. To address these issues, a standard choice is to minimise the regression error with respect to some norm. One choice is then between L^1 or L^2 (least-squares) optimisation. The former induces sparsity, which may be desirable. For instance, Mangan et al. (2016) assume the dynamics decompose in some well-chosen basis, and that most of the coefficients in the expansion vanish. They then identify a subspace to which the vector of coefficients belongs, and finally use standard algorithms to find the sparsest vector in this subspace. In Yeung, Tegnér, and Collins (2002), the authors use an SVD decomposition of some observation matrix to parametrize the set of networks consistent with the data, and then use sparse regression to find the sparsest such network. In W.-X. Wang et al. (2011), the authors decompose the dynamics over some infinite basis, then use compressed sensing to evaluate the coefficients, only few of them are then nonzero.

Least-square optimization is on the other hand less costly, and better suited for over-determined systems. In Prasse and Piet Van Mieghem (2020), the authors use a least-square optimisation, but add a L^1 penalty in order to enforce some degree of sparsity, thus solving:

$$\min_{M \in \mathcal{M}_N(\mathbb{R}^N)} \left\| \hat{Y} - M\hat{O} \right\|_2 + \lambda \|M\|_1,$$

where λ is selected by cross-validation.

Finally, let us also mention Tyrcha and Hertz (2014), which in another vein differentiates the dynamics of the model, in order to train it to reproduce the observations, as is usual for Recurrent Neural Networks.

2.3 Contributions of the article

In our work, we study the reconstruction, and prediction, problems, for an epidemic reaction-diffusion. We assume known a model, and we consider that observations are a given, standalone time-series, which is arguably the harder setting observations wise, and which seems more relevant in the case of epidemic dynamics. We first show that for almost every network, the reconstruction problem is identifiable (Lemma 6). Then, we show that the quicker the diffusion, the lower the numerical rank of the observation matrix (Corollary 8), and the harder the reconstruction, but that increasing sampling helps reconstruct the network. Then, we classify symmetrical networks generating the same trajectories (Lemma 9). Finally, we show experimentally, on synthetic data constructed with random graph generators exhibiting different topologies, that reconstruction is easier for more “constrained” topologies, and that the prediction problem can still be solved satisfyingly even when the network topology makes exact reconstruction difficult. We use least-squares under constraints to solve numerically the reconstruction problem (see Section 3.3), in the experiments.

2.4 Notations and main definitions

We use the capital letter X to designate vectors on \mathbb{R}^{3N} , for some integer $N \geq 1$, which write $X = (S, I, R)$, with $S, I, R \in \mathbb{R}^N$. Lower case x designates vectors on \mathbb{R}^3 , with $x = (s, i, r)$, and s, i and r real numbers. Whenever we consider some function f defined over \mathbb{R}^N , we choose to extend the notation in a straightforward way to \mathbb{R}^{3N} , by writing, for $X = (S, I, R)$ as above, $f(X) := (f(S), f(I), f(R))$. Whenever X is a function describing a trajectory of a dynamical system, $X : \mathbb{R}_+ \rightarrow \mathbb{R}^{3N}$, we write $Y = f(X)$ the function defined by, for all $t \geq 0$, $Y(t) := f(X(t))$. As a result, combining with what precedes, for $X = (S, I, R)$, for all $t \geq 0$, we have $Y(t) = (S(t), I(t), R(t))$. For a set $\mathcal{S} \subset \mathbb{R}^N$, for $X = (S, I, R) \in \mathbb{R}^{3N}$, we write $X \in \mathcal{S}$ to mean that S, I and R belong to \mathcal{S} . Then, for two vectors u and v of equal dimensions, we write $u \odot v$ their coordinate wise product: $u \odot v$ is the vector $(u_i v_i)_i$. Finally, 1_N designates the vector of \mathbb{R}^N with all coordinates equal to 1. Let us finally introduce the following three definitions, which help us formalise the setting.

Definition 2 (Model). *We call model, and write $\mathcal{M} = (M, (\beta, \delta), X_0)$, a tuple consisting of a diffusion matrix M , epidemiological parameters gathered in β and δ , and an initial condition $X_0 = (S_0, I_0, R_0) \in \mathbb{R}^{3N}$.*

Definition 3 (Flow on a model). *A flow Φ on the set of models \mathfrak{M} is a mapping:*

$$\begin{aligned} \Phi : \mathfrak{M} &\rightarrow \mathcal{C}(\mathbb{R}_+, \mathbb{R}^{3N}) \\ \mathcal{M} &\mapsto \Phi(\mathcal{M}) \end{aligned}$$

defined by, for each model $\mathcal{M} = (M, (\beta, \delta), X_0)$, for all $t \geq 0$, $\Phi_t(\mathcal{M})$ is the value at time t of the solution of the differential Equation (2), with initial condition X_0 , that is $\Phi_t(\mathcal{M}) = (S(t), I(t), R(t))$.

Slightly abusing notations, in the following, we sometimes write $\Phi(\mathbf{M})$ when (β, δ) and X_0 are fixed, so that the model only depends on the choice of the diffusion matrix.

Let us finally introduce the observation matrix (Tyrcha and Hertz 2014), and the vectors of estimates of the reaction terms, and the derivatives. We do not observe the whole trajectories, but only some samples of them. For some integer $K \geq 1$, let us then consider the sampling times $0 = t_0 < t_1 < t_2 < \dots < t_K$. Let for each node n $\hat{S}_n(t_k)$ be the (possibly noisy) observation of compartment S in node n at time t_k , (and likewise for the other compartments). We can also estimate the vectors of derivatives, and of reaction terms, of Equation (2), from the observations, as is done in Shandilya and Marc Timme (2011). For every $1 \leq k \leq K$, we define $\hat{\rho}_S(t_k) = \beta \hat{S}(t_k) \cdot \hat{I}(t_k)$ the vector of reaction terms on S at time t_k , and $\hat{D}_S(t_k) = \left(\hat{S}(t_k) - \hat{S}(t_{k-1}) \right) (t_k - t_{k-1})^{-1}$ the estimate of the derivative on S at time t_k . We do likewise for the other compartments.

Definition 4 (Observation matrix, derivatives and reaction terms). *Let the observation matrix on S be*

$$\hat{O}_S = \begin{pmatrix} \hat{S}_1(t_1) & \dots & \hat{S}_1(t_K) \\ \vdots & \ddots & \vdots \\ \hat{S}_N(t_1) & \dots & \hat{S}_N(t_K) \end{pmatrix} \in \mathcal{M}_{N \times K}(\mathbb{R}).$$

Note likewise \hat{O}_I the observations on I , and \hat{O}_R those on R . Define finally the matrix by block $\hat{O}((t_k), \Phi(\mathbf{M})) = \left(\hat{O}_S, \hat{O}_I, \hat{O}_R \right) \in \mathcal{M}_{N \times 3K}(\mathbb{R})$. This is the observation matrix associated with the sampling times (t_k) , and the flow $\Phi(\mathbf{M})$.

Likewise, we write $\hat{\rho}_S, \hat{D}_S \in \mathcal{M}_{N \times K}(\mathbb{R})$ the matrices of reaction terms (resp. derivatives) on S , and likewise for the other compartments. We finally define $\hat{\rho} = (\hat{\rho}_S, \hat{\rho}_I, \hat{\rho}_R) \in \mathcal{M}_{N \times 3K}(\mathbb{R})$ and $\hat{D} = \left(\hat{D}_S, \hat{D}_I, \hat{D}_R \right) \in \mathcal{M}_{N \times 3K}(\mathbb{R})$.

3 Problem Studied, Identifiability and Experimental Setup

We present the problem we address (Section 3.1), then initiate the study of its identifiability (Section 3.2), and finally present the setting in which we conduct the experiments (Section 3.3).

3.1 Problematic: Reconstruction and Prediction

We assume known the initial condition X_0 , and the epidemiological parameters β_n 's and δ_n 's. Some unknown diffusion matrix \mathbf{M}^* then generates a flow $(S, I, R) = \Phi(\mathbf{M}^*)$, and given as observations the trajectories S, I and R , we address the following two questions.

1. Question 1. Can we estimate \mathbf{M}^* from the observations? In other words, do they first uniquely define \mathbf{M}^* ? And in so, is it possible to estimate \mathbf{M}^* from them?
2. Question 2. Can we predict the future evolution of the system if, for some $T_{\text{train}} < \infty$, we can only observe the trajectories in some initial phase $0 \leq t \leq T_{\text{train}}$ of the system, that is the observations only consist in $(\Phi_t(\mathbf{M}^*), t \leq T_{\text{train}})$?

3.2 Identifiability of the Diffusion

We now conduct some preliminary analysis on the identifiability of the diffusion. We have the following characterisation of the set of diffusion matrices \mathbf{M} which

produce the same trajectories as M^* (see Appendix A for a proof, and likewise for future results).

Lemma 5 (Diffusions Generating the Same Trajectories). *Let M^* be a diffusion matrix, and write $(S, I, R) = \Phi(M^*)$. Then, every matrix $M = M^* + H$, such that first M is a diffusion matrix, and secondly such that for all $t \geq 0$, we have⁴ $\Phi_t(M) \in \ker H$, produces the same trajectories as M^* .*

As a result, provided the vector space generated by the trajectories, that is by the vectors $S(t)$, $I(t)$ and $R(t)$, for $t \geq 0$, is the whole space \mathbb{R}^N , then the answer to our first question is affirmative (as the only H possible vanishes over the whole space, therefore vanishes). Therefore, a fundamental question governing the issue of the identifiability of the diffusion matrix is the existence of strict subspaces of \mathbb{R}^N in which the trajectories evolve. This moreover gives us a practical criterion to evaluate if the diffusion matrix generating a given trajectory is unique: we check if the observation matrix has rank N , which is sufficient to guarantee the uniqueness. Now, often the trajectories generate the whole space, as the next result shows.

Lemma 6 (Almost Everywhere Identifiability). *Let $0 \leq t_1 < \dots < t_N < \infty$ be a subdivision of the nonnegative real half-axis. Then, for almost every M , X_0 , for all β , δ , writing $\mathcal{M} = (M, (\beta, \delta), X_0)$, the space generated by the samples of the trajectories at instants t_1, \dots, t_N (that is $\Phi_{t_1}(\mathcal{M}), \dots, \Phi_{t_N}(\mathcal{M})$), is equal to \mathbb{R}^N .*

This might give the impression the problem is solved, for almost every M and X_0 . Indeed, assume the space generated by the trajectories is the whole of \mathbb{R}^N . Then, the observation matrix $\hat{O}((t_k), \Phi(M))$ has rank N . We therefore know the image of M on a basis, which fully determines it. However, the conditioning of the observation matrix is often poor in practice, so that reconstruction of M^* by extracting a basis is inefficient. In the next two sections, we investigate two reasons why this is the case. Firstly, we study the influence of the speed of diffusion in Section 4. Secondly, we consider the topology of the graph in Section 5. Nonetheless, the fact the diffusion is often unique means that, when running a reconstruction algorithm, we can have good hope it will succeed in finding a good fit, which we show is the case in the experiments.

3.3 Experimental Set-Up

For each experiment, we start by generating a graph from a random graph generator. We use four random graphs, with different topologies: the Erdős-Rényi and the Waxman graph, which are quite connected graphs, and therefore quite “close” to a complete graph, and the Relaxed Caveman and extended Barabási-Albert graphs, which are less connected, and exhibit a more clustered structure. In that sense, the diffusion is more constrained by these graphs, and we expect the reconstruction problems to be easier in that case. We study graphs of sizes ranging from $N = 20$ to $N = 140$. Then, we draw the coefficients of the diffusion matrix M^* uniformly on $[0, 1]$. Finally, when needed, we renormalise the diffusion matrix by the typical time of diffusion $\tau > 0$. The epidemiological coefficients β_n and δ_n are drawn at random, such that for each node n , we have $\beta_n \sim |\mathcal{N}(1, 2)|$ and $\delta_n \sim |\mathcal{N}(3 \times 10^{-2}, 6 \times 10^{-2})|$.

Next, we simulate the ground truth trajectories on the time interval $[0, T_\infty]$, with $T_\infty = 10$. We use a uniform time discretisation step of $(\Delta t)_{\text{groundtruth}} = 10^{-3}$, and a Runge-Kutta discretisation scheme of order 4. For each setting, we repeat the experiments at least 5 times, so as to control the stochastic fluctuations. Finally, the train set in which we sample the observations is $[0, T_{\text{train}}]$, with $T_{\text{train}} = 2$. We use various sample steps $(\Delta t)_{\text{sample}}$, ranging between 2×10^{-3} and 10^{-2} . Recall from Section 2.1 that we write $\tilde{\mu}_M$ the stationary distribution of the diffusion matrix M . In each experiment, we use as initial condition

⁴As explained in Section 2.4, $\Phi_t(M) \in \ker H$ means that $S(t)$, $I(t)$ and $R(t)$ belong to $\ker H$.

$X_0 = (S(0), I(0), R(0)) = (s_0\tilde{\mu}_M, i_0\tilde{\mu}_M, r_0\tilde{\mu}_M)$, where s_0 , i_0 and r_0 are nonnegative real numbers, and $i_0 > 0$. As a result, the vector of initial susceptibles $S(0)$ is proportional to the stationary distribution, and likewise for $I(0)$ and $R(0)$. We compute the reconstructed diffusion matrix by solving

$$\min_{M \in \mathcal{M}_N(\mathbb{R})} \left\| \hat{D} - \hat{R} - M\hat{O} \right\|_2,$$

such that $\begin{cases} M_{i,j} \geq 0, i \neq j, \\ \sum_j M_{i,j} = 0 \text{ for all node } i. \end{cases}$

This is a convex optimisation problem. We solved it using the Python package CVXPY (Diamond and Boyd 2016; Agrawal et al. 2018). We write M_{rec} the matrix obtained. Moreover, to truly enforce the fact M_{rec} is a diffusion matrix, we post-processed the matrix obtained by enforcing that column sums vanish: for every node n , we replaced the diagonal coefficient $M_{\text{rec}}(n, n)$ by $-\sum_{i=1}^N M_{\text{rec}}(i, n)$.

To assess the reconstruction, we use two metrics. First, we use the AUC (Fawcett 2006) on the presence of edges, as Prasse and Piet Van Mieghem (2020). It is computed thanks to the corresponding function in Scikit-learn (Pedregosa et al. 2011). Secondly, we evaluate the prediction error, that is the norm of the difference between the trajectories computed with the true model, and those computed with the reconstructed diffusion M_{rec} , by

$$\frac{1}{N} \frac{1}{T_\infty - T_{\text{train}}} \sum_{p=1}^{p_{\max}} \left\| \Phi_{t_p}(M^*) - \Phi_{t_p}(M_{\text{rec}}) \right\|^2 (t_p - t_{p-1}), \quad (3)$$

where $p_{\max} = \lfloor \frac{T_\infty - T_{\text{train}}}{(\Delta t)_{\text{groundtruth}}} \rfloor$ and (t_p) is the discretisation scheme used for the simulations, whose beginning has been removed, so that $t_0 = T_{\text{train}}$.

Computations with the Barabási-Albert graph were prone to numerical instabilities. We believe this is due to its topology being more constrained. As a result, we modified a bit the experimental setting for this specific graph, increasing sampling to $(\Delta t)_{\text{sample}} = 4 \times 10^{-3}$, and increasing the number of repetitions to 30.

4 Influence of the Diffusion Rate

We now study the influence of the diffusion rate on the feasibility of the network reconstruction, first theoretically (Section 4.1), then experimentally (Section 4.2).

4.1 Analysis

One difficulty of the network reconstruction problem is the conditioning of the observation matrix (Definition 4), which may be poor. In particular, its numerical rank may be significantly lower than N , as observed also in (Prasse and Piet Van Mieghem 2020). In our case, this may be partly due to the homogenisation performed by the diffusion. Indeed, given different epidemiological parameters, and different population sizes, the internal dynamics of the different nodes evolve differently. However, the diffusion tends to homogenise each compartment, so that $S(t)$ tends to a vector proportional to the stationary distribution, $\tilde{\mu}_M$, and likewise for $I(t)$ and $R(t)$. As a result, the diffusion tends to worsen the conditioning of a basis. This effect depends on the time-scale at which diffusion occurs, with respect to that at which the reactions in each node occur. We first show, in the following Lemma 7, that when the typical time of evolution of the diffusion, τ , goes to 0 (equivalently, the diffusion rate $1/\tau$ goes to infinity), and in the presence of fixed epidemiological parameters, the trajectories tend to those of a scalar SIR systems, which coefficients we express in terms of the β_n 's, the δ_n 's and the stationary

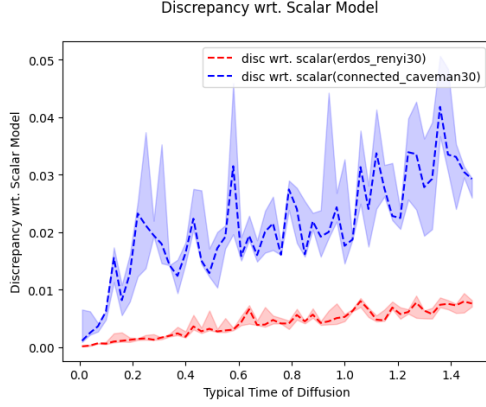


Figure 1: Discrepancy between the Scalar Model and the True Model as a Function of the Typical Time of Diffusion

distribution, times the stationary distribution for each compartment. We then address the consequences for the numerical rank in Corollary 8. For any $\tau > 0$, we write $\Phi^\tau = \Phi\left(\frac{M}{\tau}\right)$, that is the flow obtained by replacing M by M/τ in Equation (2).

Lemma 7 (Limit Trajectories for Diffusion Rate going to Infinity). *Let $\mathcal{M} = (M, (\beta, \delta), X_0)$ be a model, and assume the initial condition X_0 is such that S_0, I_0 and R_0 are proportional to the stationary distribution $\tilde{\mu}_M$. Write (s, i, r) the solutions of the scalar system*

$$\begin{cases} \frac{ds}{dt} = -\tilde{\beta}si \\ \frac{di}{dt} = \tilde{\beta}si - \tilde{\delta}i \\ \frac{dr}{dt} = \tilde{\delta}i, \end{cases}$$

with $s(0) = \sum_n S_n(0)$, and likewise for i and r , and with

$$\tilde{\beta} = \sum_n \beta_n \tilde{\mu}_M(n)^2, \quad \text{and} \quad \tilde{\delta} = \sum_n \delta_n \tilde{\mu}_M(n).$$

Then, for any $T > 0$, $\Phi^\tau(\mathcal{M}) \rightarrow (s\tilde{\mu}_M, i\tilde{\mu}_M, r\tilde{\mu}_M)$, as $\tau \rightarrow 0$, uniformly on $[0, T]$.

We illustrate Lemma 7 on Figure 1. We ran experiments according to the protocol described in Section 3.3, using Erdős-Rényi and Relaxed Caveman graphs, for a range of values of τ . For (t_p) the discretisation scheme used for the simulations, and p_{\max} the number of t_p 's, we plot the error

$$\frac{1}{N} \frac{1}{T_\infty} \sum_{p=1}^{p_{\max}} \left\| \Phi_{t_p}\left(\frac{M}{\tau}\right) - (s(t_p)\tilde{\mu}_M, i(t_p)\tilde{\mu}_M, r(t_p)\tilde{\mu}_M) \right\|_2^2 (t_p - t_{p-1})$$

between the trajectories obtained with the vector model, and those computed from the scalar model. We indeed see it goes to 0, as $\tau \rightarrow 0$. Moreover, the discrepancy is bigger for the Relaxed Caveman graph, than for the Erdős-Rényi one: indeed, the latter is more connected, and therefore there are much more exchanges between the nodes, so that it is closer to a kind of “average” model, which the scalar limit is. Then, from Lemma 7, we immediately have the following corollary which describes its consequences for the numerical rank of the observation matrix.

Corollary 8 (Numerical Rank of the Observation Matrix for Diffusion Rate going to Infinity). *We make the same assumptions as in Lemma 7. Let, for some integer $K \geq 1$, $(t_k)_{1 \leq k \leq K}$ be a family of sample times. Let $\tau > 0$, and let us*

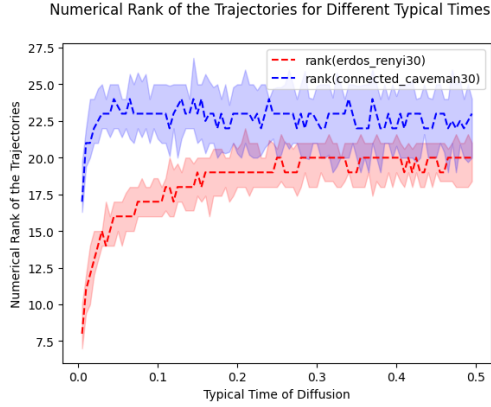


Figure 2: Numerical rank, of the observation matrix, for a fixed family of sample times, and two random graphs of 30 nodes, for various diffusion rates τ .

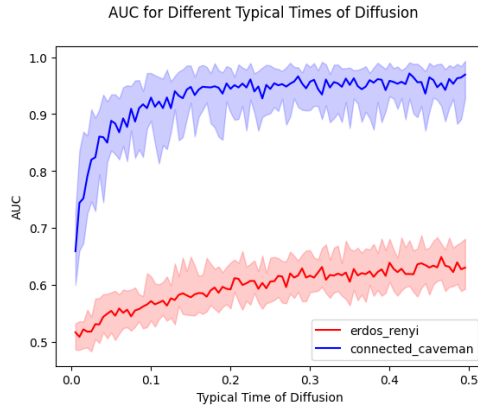


Figure 3: AUCs for Various Diffusion Rates

write $\hat{O}((t_k), \Phi^\tau(M))$ the observation matrix associated with the t_k 's, and the flow $\Phi^\tau(M)$. Then, the numerical rank of the matrix $\hat{O}((t_k), \Phi^\tau(M))$ goes to 1, as $\tau \rightarrow 0$.

We illustrate this convergence on Figure 2. We use the same protocol as for Figure 1, but this time display the numerical rank. We see it gets lower and lower, as $\tau \rightarrow 0$. It is lower for the Erdős-Rényi graph, probably for the same reasons given above.

4.2 Experiments: Diffusion Rate, Sampling Frequency

Let us now investigate the consequences of this phenomenon, for the practical reconstruction problem. We first show on Figure 3 the AUC as a function of the typical time of diffusion τ , for a fixed sampling rate. The AUC increases as the typical time of diffusion decreases, as we expected. It is bigger for the Relaxed Caveman graph, which has “more structure” than the Erdős-Rényi one. Then, we study how increased sampling may help prediction for high diffusion rates. We therefore ran experiments for different values of τ , and different sampling rates. On Figure 4, we show a heatmap of the AUC, with different sampling steps, and diffusion rates, for an Erdős-Rényi graph of 30 nodes. The darker the color, the smaller the AUC is. On each row, we see colors get darker as we go to the right: this means that, for each fixed diffusion rate, the AUC deteriorates as the sampling step increases. On each column, we see colors get darker as we move to the top:

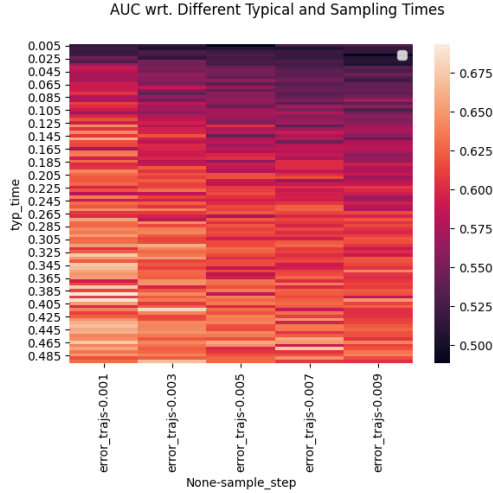


Figure 4: Heatmap of AUCs wrt. Typical Time of Diffusion and Sampling Step

this means that, for each sampling step, the AUC worsens as the diffusion rate increases. Overall, we see that the bottom left triangle is lighter (sampling is high enough with respect to the diffusion rate, AUCs are big), while the top right triangle is darker (sampling is low with respect to the diffusion rate, AUCs are lower).

5 Influence of the Network Topology

We now study the influence of the network topology, first theoretically, from an algebraic standpoint (Section 5.1), then experimentally (Section 5.2).

5.1 Symmetries

Thanks to Lemma 5 we know that identifiability of M is linked to the dimension of the vector space spanned by the flow $\Phi(\mathcal{M})$. Now, symmetries of the model may cause the trajectories to live in low dimensional spaces. Indeed, they often lower the dimensions of the studied spaces by eliminating the dependencies of equations in some variables. For instance, a 2 dimensional problem in physics which is invariant under rotations around the origin will have a solution which will only depend on the distance to the origin. These principles have been applied successfully to numerous fields, and have been used in the context of mathematical epidemiology (Simon, Taylor, and Kiss 2011; Ward and López-García 2019) to reduce the number of calculations needed to simulate the propagation of diseases. We now investigate the influence of symmetries on the inverse problem we study.

Let us first define precisely symmetries. We write \mathfrak{S}_N the symmetric group of order N , and σ its elements, which are called permutations. We write $P(\sigma)$ the permutation matrix associated to the permutation σ . Then, for any $V \in \mathbb{R}^N$, $P(\sigma)V = V$ if, and only if, for every orbit of σ , for every i, j in this orbit, we have $V_i = V_j$. A vector $X = (S, I, R)$ is symmetric with respect to σ if $P(\sigma)S = S$, and likewise for I and R . This notion extends to groups of permutations, as follows. Let \mathcal{H} be a subgroup of \mathfrak{S}_N , and define $\text{Fix}(\mathcal{H})$ (Lang 2012) the space of vectors stable by \mathcal{H} , that is:

$$\text{Fix}(\mathcal{H}) = \{V \in \mathbb{R}^N \mid \forall \sigma \in \mathcal{H}, P(\sigma)V = V\}.$$

Then, X is said to be symmetric with respect to \mathcal{H} if $X \in \text{Fix}(\mathcal{H})$. This extends to flows by saying that a flow $(S, I, R) = \Phi(\mathcal{M})$ is symmetric with respect to \mathcal{H} if

$\Phi(\mathcal{M}) \in \text{Fix}(\mathcal{H})$. Finally, we say that a model $\mathcal{M} = (M, (\beta, \delta), X_0)$ is symmetric with respect to some permutation σ if, writing $P = P(\sigma)$, we have $M = PMP^{-1}$, $P\beta = \beta$, $P\delta = \delta$ and $PX_0 = X_0$. We then say σ is an automorphism of \mathcal{M} , extending in a straightforward way the notion of graph automorphism (Hell and Nesetril 2004). Indeed, if σ is an automorphism of \mathcal{M} , then it is in particular an automorphism of the underlying weighted graph, meaning that for all nodes $i, j \in \mathcal{N}$, the edges $i \rightsquigarrow j$ and $\sigma(i) \rightsquigarrow \sigma(j)$ have the same weight: $M_{i,j} = M_{\sigma(i),\sigma(j)}$. We write $\text{Aut}(\mathcal{M})$ the group of model automorphisms of \mathcal{M} .

We first establish, in Lemma 9, that trajectories generated by a diffusion M are symmetrical with respect to some group \mathcal{H} first if, and only if, there exists a diffusion admitting all permutations in \mathcal{H} as automorphisms which generates the same trajectories and secondly if, and only if, the diffusion M stabilizes $\text{Fix}(\mathcal{H})$.

Lemma 9 (Networks Generating Symmetrical Trajectories). *Let M be a diffusion matrix, β, δ be the vectors of epidemiological coefficients, and \mathcal{H} be a subgroup of \mathfrak{S}_N . Assume that β and δ are symmetric with respect to \mathcal{H} . Then, the following conditions are equivalent.*

1. *Symmetries of the Trajectories.* For all $X_0 \in \text{Fix}(\mathcal{H})$, the flow of $(M, (\beta, \delta), X_0)$ is symmetric with respect to \mathcal{H} .
2. *Symmetrical Generating Diffusion.* There exists a diffusion matrix \bar{M} such that $\mathcal{H} \subset \text{Aut}(\bar{M}, (\beta, \delta), X_0)$ and such that for all $X_0 \in \text{Fix}(\mathcal{H})$, the flow of $(\bar{M}, (\beta, \delta), X_0)$ equals the flow of $(M, (\beta, \delta), X_0)$.
3. *Stabilization by the Diffusion.* M stabilizes $\text{Fix}(\mathcal{H})$, that is $M\text{Fix}(\mathcal{H}) \subset \text{Fix}(\mathcal{H})$.

We now show that, in the spirit of Lemma 5, trajectories symmetrical with respect to \mathcal{H} are generated by diffusions which differ by a matrix Z vanishing on $\text{Fix}(\mathcal{H})$. These matrices represent the fact flows between nodes with identical S , I and R values may be redirected freely within themselves, provided the outgoing flows are modified accordingly⁵. The nodes where the flows are identical are those in the same orbits under \mathcal{H} (Lang 2012), that is the nodes i and j such that, for some $\sigma \in \mathcal{H}$, we have $j = \sigma(i)$. Define therefore, for all $1 \leq i < j \leq N$, and for all $1 \leq k \leq N - 1$, the redirection matrix

$$Z^{i,j,k} = E_{k,i} - E_{k,j} - E_{N,i} + E_{N,j},$$

where the $E_{r,s}$'s matrices are the vectors of the canonical basis of $\mathcal{M}_N(\mathbb{R})$. This matrix removes one unit of rate from the edge $j \rightsquigarrow k$, and adds one unit of rate on the edge $i \rightsquigarrow k$. It does the reverse with respect to the node N , taking one unit of rate from $i \rightsquigarrow N$ and adding it to $j \rightsquigarrow N$, in order to enforce the fact that the sums of $Z^{i,j,k}$ vanish, that is as much rate goes to each node than goes out.

Lemma 10 (Flow Redirection within the Orbits). *Under the same assumptions as in Lemma 9, let \mathcal{H} be the biggest group of symmetries letting invariant the trajectories. Then, the affine space of matrices producing the same trajectories as M for every initial condition $X_0 \in \text{Fix}(\mathcal{H})$ is exactly the subspace generated by the $Z^{i,j,k}$'s, for all i and j which are in the same orbit under \mathcal{H} . This space has dimension at least*

$$(N - 1)(N - \#\{\text{different trajectories}\}).$$

The dimension of this space is a lower bound on the dimension of the affine space of matrices generating the same trajectories as M . To summarize, given a diffusion matrix M , we have given an explicit description of a set of matrices giving

⁵In fact, Z matrices, like the diffusion matrices, describe rates. However, as long as nodes have equal values, modifying the rates, or the flows going out of them, becomes equivalent.

the same trajectories as M . As a result, if the diffusion matrix we try to reconstruct gives symmetrical trajectories, and if we have an algorithm which gives us one solution of the reconstruction problem, then we are able to find many such matrices explicitly, though we cannot single the original M out. Note that this has consequences on the conditioning of the observation matrix. Indeed, its rank is then necessarily bounded by $\#\{\text{different trajectories}\}$. As such, if the model presents symmetries, then several singular values of the observation matrix will be zero, and in a neighbourhood of M as well, the numerical rank will be bounded by $N - \#\{\text{different trajectories}\}$. This proves that the nearest a model is to a symmetrical model, the most difficult it is to reconstruct the diffusion matrix.

5.2 Network Topology Experiments

We now study experimentally the influence of the network topology on the estimation and prediction problems. As explained in Section 3.3, we study two metrics: the AUC on the presence or absence of edges, and the prediction error, and we present results for various sizes of graphs, and various types of random networks, exhibiting different topologies. The plots are box plots, where the solid lines are the medians of values, and the shaded areas gather the [10%, 90%] intervals of values.

We present, on Figure 5, the AUC as a function of the number of nodes, for various types of random graphs. The full set of parameters used is available in the code. The AUC is quite good for small graphs, more than 0.8, but decreases as the number of nodes increases. As expected, the more constrained the topology, the better the AUC. Indeed, it is in general best for the Barabási-Albert graph, and the second best is often the Relaxed Caveman graph. The Waxman graph, and above all the Erdős-Rényi one, exhibit the worse AUCs.

On Figure 6, we show the prediction error. We see the prediction errors in general are quite low, less than 2×10^{-4} , and diminish with the number of nodes. Moreover, the Erdős-Rényi graph consistently exhibits the lowest error. These results are consistent with each other, in the sense that it seems the more the graph has connections, the easiest it is to predict the future behaviour of the system (more edges, either through more nodes, or through the topology, in the case of the Erdős-Rényi graph). However, they are opposite to the results for the AUCs. Therefore, they tend to suggest that the more constrained the topology, the easier it is to reconstruct the network, but the more mixing there is, the easiest it is to predict the future evolution of the system. We did not display the prediction errors for the Barabási-Albert graph, as it was about 5 times greater than for the other graphs, and exhibited also high variance. We believe it comes probably first from the fact it is prone to numerical instabilities, as we said in Section 3.3. Secondly, it is also probably due to its topology being more constrained: as a result, small errors on the reconstruction lead to high errors on the prediction.

Finally, on Figure 7, we see the numerical rank of the observation matrix for several graphs. It tends to stagnate or decrease as the number of nodes increases, which is not surprising, as large matrices tend to have small singular values, which therefore do not contribute to the numerical rank. It is consistently higher for the Barabási-Albert graph, which structure is more constrained.

6 Conclusions, future works

In this article, we have studied the reconstruction, and prediction, problems, for an epidemic reaction-diffusion. We have proved that for almost every network, the reconstruction problem is identifiable. Then, we have shown that the quicker the diffusion, the lower the numerical rank of the observation matrix, and the harder the reconstruction, but that increasing sampling helped reconstruct the network.

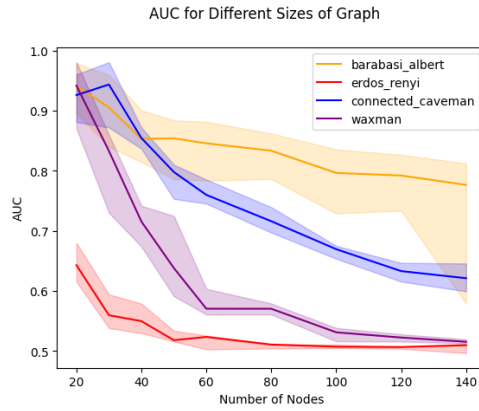


Figure 5: AUC on the Adjacency Matrix for Various Graphs and Sizes of Graphs

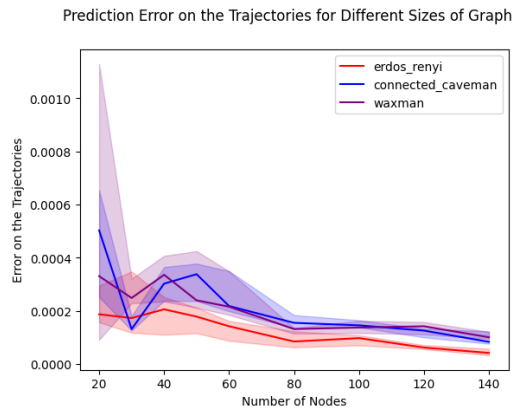


Figure 6: Prediction Error on the Trajectories for Various Sizes of Graphs

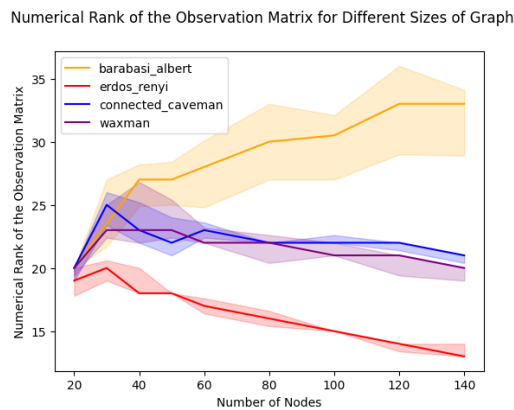


Figure 7: Numerical Ranks of the Observation Matrix for Various Sizes of Graphs

Then, we have classified symmetrical networks generating the same trajectories. Finally, we showed experimentally, on synthetic data constructed with random graph generators exhibiting different topologies, that reconstruction was easier for more “constrained” topologies, and that the prediction problem could still be solved satisfyingly even when the network topology makes exact reconstruction difficult.

We have studied the case when the observations we have consist of all the trajectories in all the nodes. Other studies have considered partial observations, as in the presence of missing nodes (Tyrcha and Hertz 2014; Haehne et al. 2019), or more generally partial observations (Nitzan, Casadiego, and Timme 2017; Ioannidis, Romero, and Giannakis 2018; Ioannidis, Shen, and Giannakis 2019). This would be an interesting extension to further our work.

Then, measures often come with a level of noise, and studying the robustness of reconstruction in the presence of noise should be another direction of study.

Finally, studies on real-world data would allow to attempt at separating the specific influence of diffusion, through transportation networks for instance, on the spread of epidemics, from that of internal (within cities, or countries) reactions.

References

- [Agr+18] Akshay Agrawal et al. “A rewriting system for convex optimization problems”. In: *Journal of Control and Decision* 5.1 (2018), pp. 42–60 (cit. on p. 8).
- [All+07] L. J. S. Allen et al. “Asymptotic Profiles of the Steady States for an SIS Epidemic Patch Model”. In: *SIAM Journal of Applied Mathematics* 67 (5 2007), pp. 1283–1309 (cit. on pp. 2, 3).
- [Ari09] Julien Arino. “Diseases in Metapopulations”. In: *Modeling and Dynamics of Infectious Diseases* (2009), pp. 64–122 (cit. on pp. 2, 3).
- [Ari17] Julien Arino. “Spatio-temporal spread of infectious pathogens of humans”. In: *Infectious Disease Modelling* (2 2017), pp. 218–228 (cit. on pp. 2, 3).
- [BB13] B. Barzel and A.-L. Barabási. “Network link prediction by global silencing of indirect correlations”. In: *Natural Biotechnologies* 31 (2013), pp. 720–725 (cit. on p. 4).
- [BD01] Fred Brauer and P. van den Driessche. “Models for transmission of disease with immigration of infectives”. In: *Mathematical Biosciences* 171 (2 June 2001), pp. 143–154 (cit. on pp. 2, 3).
- [BKT11] F. van Bussel, B. Kriener, and M. Timme. “Inferring synaptic connectivity from spatio-temporal spike patterns”. In: *Frontiers in Computational Neurosciences* 5 (3 Feb. 2011) (cit. on p. 4).
- [Cas+17] Jose Casadiego et al. “Model-free inference of direct network interactions from nonlinear collective dynamics”. In: *Nature Communications* (2017) (cit. on p. 4).
- [DB16] Steven Diamond and Stephen Boyd. “CVXPY: A Python-embedded modeling language for convex optimization”. In: *Journal of Machine Learning Research* 17.83 (2016), pp. 1–5 (cit. on p. 8).
- [DHB12] Odo Diekmann, Hans Heesterbeek, and Tom Britton. *Mathematical Tools for Understanding Infectious Disease Dynamics*. Princeton series in theoretical and computational biology. 2012 (cit. on pp. 1–3).
- [DHR09] O. Diekmann, J. A. P. Heesterbeek, and M. G. Roberts. “The construction of next-generation matrices for compartmental epidemic models”. In: *Journal of The Royal Society* (2009). DOI: [10.1098/rsif.2009.0386](https://doi.org/10.1098/rsif.2009.0386) (cit. on p. 3).

- [Don+15] Xiaowen Dong et al. “Laplacian matrix learning for smooth graph signal representation”. In: *2015 IEEE International Conference on Acoustics, Speech and Signal Processing (ICASSP)* (2015), pp. 3736–3740 (cit. on p. 1).
- [Dur10] Rick Durrett. “Some features of the spread of epidemics and information on a random graph”. In: *Proceedings of the National Academy of Sciences* 107.10 (2010), pp. 4491–4498. ISSN: 0027-8424. DOI: [10.1073/pnas.0914402107](https://doi.org/10.1073/pnas.0914402107). eprint: <https://www.pnas.org/content/107/10/4491.full.pdf>. URL: <https://www.pnas.org/content/107/10/4491> (cit. on p. 2).
- [Faw06] Tom Fawcett. “An introduction to ROC analysis”. In: *Pattern Recognition Letters* 27.8 (2006). ROC Analysis in Pattern Recognition, pp. 861–874. ISSN: 0167-8655. DOI: <https://doi.org/10.1016/j.patrec.2005.10.010>. URL: <https://www.sciencedirect.com/science/article/pii/S016786550500303X> (cit. on p. 8).
- [Gar+03] T. Gardner et al. “Inferring Genetic Networks and Identifying Compound Mode of Action via Expression Profiling”. In: *Science* 301 (5629 July 2003), pp. 102–105 (cit. on pp. 1, 4).
- [GMT05] A. Ganesh, L. Massoulié, and D. Towsley. “The effect of network topology on the spread of epidemics”. In: *Proceedings IEEE 24th Annual Joint Conference of the IEEE Computer and Communications Societies*. 2 (2005), 1455–1466 vol. 2 (cit. on p. 2).
- [Hae+19] Hauke Haehne et al. “Detecting Hidden Units and Network Size from Perceptible Dynamics”. In: *Phys. Rev. Lett.* 122 (15 Apr. 2019), p. 158301. DOI: [10.1103/PhysRevLett.122.158301](https://doi.org/10.1103/PhysRevLett.122.158301). URL: <https://link.aps.org/doi/10.1103/PhysRevLett.122.158301> (cit. on pp. 2, 15).
- [HG97] I. A. Hanski and M.E. Gilpin. *Metapopulation Biology: Ecology, Genetics, and Evolution*. Academic Press, 1997 (cit. on p. 1).
- [HN04] P. Hell and J. Neseřtil. *Graphs and Homomorphisms*. Oxford Lecture Series in Mathematics and Its Applications. OUP Oxford, 2004. ISBN: 9780198528173. URL: <https://books.google.fr/books?id=bJXWV-qK7kYC> (cit. on p. 12).
- [IRG18] Vassilis N. Ioannidis, Daniel Romero, and Georgios B. Giannakis. “Inference of Spatio-Temporal Functions Over Graphs via Multikernel Kriged Kalman Filtering”. In: *IEEE Transactions on Signal Processing* 66.12 (2018), pp. 3228–3239. DOI: [10.1109/TSP.2018.2827328](https://doi.org/10.1109/TSP.2018.2827328) (cit. on p. 15).
- [ISG19] Vassilis N. Ioannidis, Yanning Shen, and Georgios B. Giannakis. “Semi-Blind Inference of Topologies and Dynamical Processes Over Dynamic Graphs”. In: *IEEE Transactions on Signal Processing* 67 (9 May 2019) (cit. on p. 15).
- [KM27] William Ogilvy Kermack and A.G. McKendrick. “A contribution to the mathematical theory of epidemics”. In: *Journal of The Royal Society* (1927) (cit. on p. 1).
- [KS08] G. Karlebach and R. Shamir. “Modelling and analysis of gene regulatory networks”. In: *Nature Review of Molecular Cellular Biology* 9 (2008), pp. 770–780 (cit. on p. 1).
- [Lan12] S. Lang. *Algebra*. Graduate Texts in Mathematics. Springer New York, 2012. ISBN: 9781461265511. URL: <https://books.google.fr/books?id=Yt7LnQEACAAJ> (cit. on pp. 11, 12, 20).
- [Le +19] Batiste Le Bars et al. “Learning Laplacian Matrix from Bandlimited Graph Signals”. In: *ICASSP 2019 - 2019 IEEE International Conference on Acoustics, Speech and Signal Processing (ICASSP)*. 2019, pp. 2937–2941. DOI: [10.1109/ICASSP.2019.8682769](https://doi.org/10.1109/ICASSP.2019.8682769) (cit. on p. 1).
- [Man+16] N. M. Mangan et al. “Inferring biological networks by sparse identification of nonlinear dynamics”. In: *IEEE Transactions on Molecular,*

- Biological and Multi-Scale Communications* 2 (2016), pp. 52–63 (cit. on p. 4).
- [Mey00] Carl D. Meyer. *Matrix Analysis and Applied Linear Algebra*. Society for Industrial and Applied Mathematics Philadelphia, PA, USA, 2000 (cit. on p. 3).
- [MPF05] V. Makarov, F. Panetsos, and O. de Feo. “A method for determining neural connectivity and inferring the underlying networks dynamics using extracellular spike recordings”. In: *Journal of Neurosciences Methods* 144 (2 2005), pp. 265–279 (cit. on p. 4).
- [NCT17] Mor Nitzan, Jose Casadiego, and Marc Timme. “Revealing physical interaction networks from statistics of collective dynamics”. In: *Science Advances* 3 (Feb. 2017) (cit. on p. 15).
- [NPP16] Cameron Nowzari, Victor M. Preciado, and George J. Pappas. “Analysis and Control of Epidemics: A survey of spreading processes on complex networks”. In: *IEEE Control Systems Magazine* (2016) (cit. on pp. 1, 3).
- [NWS02] M. E. J. Newman, D. J. Watts, and S. H. Strogatz. “Random graphs of social networks”. In: *Proc. Natl. Acad. Sci. USA* 99 (1 2002), pp. 2566–2572 (cit. on p. 1).
- [Pas+15] R. Pastor-Satorra et al. In: *Review of Modern Physics* 87 (3 2015), pp. 925–979 (cit. on p. 1).
- [PDV21] Bastian Prasse, Karel Devriendt, and Piet Van Mieghem. “Clustering for epidemics on networks: a geometric approach”. In: *preprint* (2021) (cit. on p. 2).
- [Ped+11] F. Pedregosa et al. “Scikit-learn: Machine Learning in Python”. In: *Journal of Machine Learning Research* 12 (2011), pp. 2825–2830 (cit. on p. 8).
- [Per+17] Domenico Perfido et al. “Towards Sustainable Water Networks: Automated Fault Detection and Diagnosis”. In: *THE International Journal of Entrepreneurship and Sustainability Issues* 4 (3 Mar. 2017) (cit. on p. 1).
- [PV01] R. Pastor-Satorras and A. Vespignani. In: *Physical Review Letter* 86 (14 2001) (cit. on p. 1).
- [PV04] R. Pastor-Satorras and A. Vespignani. *Internet: structure et évolution*. Belin, 2004 (cit. on p. 1).
- [PV20] Bastian Prasse and Piet Van Mieghem. “Network Reconstruction and Prediction of Epidemic Outbreaks for General Group-Based Compartmental Epidemic Models”. In: *IEEE Transactions on Network Science and Engineering* 7 (4 2020) (cit. on pp. 1, 2, 4, 5, 8).
- [Qui+11] C. J. Quinn et al. “Estimating the directed information to infer causal relationships in ensemble neural spike train recordings”. In: *Journal of Computational Neurosciences* 30 (2011), pp. 17–44 (cit. on p. 4).
- [SB93] J. Stoer and R. Burlisch. *Introduction to Numerical Analysis*. New York: Springer, 1993 (cit. on p. 4).
- [SBL19] Stefania Sardellitti, Sergio Barbarossa, and Paolo Di Lorenzo. “Graph Topology Inference Based on Sparsifying Transform Learning”. In: *IEEE Transactions on Signal Processing* 67.7 (Apr. 2019), pp. 1712–1727. DOI: [10.1109/TSP.2019.2896229](https://doi.org/10.1109/TSP.2019.2896229). arXiv: [1806.01701](https://arxiv.org/abs/1806.01701) [eess.SP] (cit. on p. 1).
- [SSV13] F. D. Sahneh, C. Scoglio, and P. Van Mieghem. “Generalize epidemic mean-field model for spreading processes over multilayer complex networks”. In: *IEEE/ACM Transactions on Networking* 21 (5 Oct. 2013), pp. 1609–1620 (cit. on p. 1).
- [ST11] Srinivas Gorur Shandilya and Marc Timme. “Inferring network topology from complex dynamics”. In: *New Journal of Physics* 13 (2011) (cit. on pp. 1, 4, 6).

- [STK11] P. L. Simon, M. Taylor, and I. Z. Kiss. “Exact epidemic models on graphs using graph-automorphism driven lumping”. In: *Journal of Mathematical Biology* 62 (4 2011), pp. 479–508 (cit. on pp. 2, 11).
- [Sut04] Wilson Alexander Sutherland. *Introduction to Metric and Topological Spaces*. Oxford University Press, 2004 (cit. on p. 23).
- [TC14] Marc Timme and Jose Casadiego. “Revealing networks from dynamics: an introduction”. In: *Journal of Physics A: Mathematical and Theoretical* 47 (2014) (cit. on pp. 1, 2, 4).
- [TH14] Joanna Tyrcha and John Hertz. “Network Inference with Hidden Units”. In: *Mathematical Biosciences and Engineering* 11 (1 Feb. 2014), pp. 149–165 (cit. on pp. 5, 6, 15).
- [Tie+15] Joseph H. Tien et al. “Disease invasion on community networks with environmental pathogen movement”. In: *Journal of Mathematical Biology* 70 (2015), pp. 1065–1092 (cit. on pp. 2, 3).
- [TOM19] Natascia Tamburello, Brian O. Ma, and Isabelle M. Côté. “From individual movement behaviour to landscape-scale invasion dynamics and management: a case study of lionfish metapopulation”. In: *Philosophical Transactions of the Royal Society B* 374 (Mar. 2019) (cit. on p. 1).
- [VS18] Aram Vajdi and Caterina Scoglio. “Identification of Missing Links Using Susceptible-Infected-Susceptible Spreading Traces”. In: *IEEE Transactions on Network Science and Engineering* 6 (4 2018), pp. 917–927 (cit. on p. 2).
- [VW02] P. Van den Driessche and J. Watmough. “Reproduction numbers and sub-threshold endemic equilibria for compartmental models of disease transmission”. In: *Mathematical Biosciences* (2002). DOI: [https://doi.org/10.1016/S0025-5564\(02\)00108-6](https://doi.org/10.1016/S0025-5564(02)00108-6) (cit. on pp. 2, 3).
- [Wan+11] W.-X. Wang et al. “Time-series based prediction of complex oscillator networks via compressive sensing”. In: *Europhys. Lett.* 94 (2011) (cit. on p. 4).
- [WL19] J. A. Ward and López-García. “Exact analysis of summary statistics for continuous-time discrete-state Markov processes on networks using graph-automorphism lumping”. In: *Applied Network Science* 4 (1 2019) (cit. on pp. 2, 11).
- [WZ05] Wendi Wang and Xiao-Qiang Zhao. “An Age-Structured Epidemic Model in a Patchy Environment”. In: *SIAM Journal on Applied Mathematics* 65 (5 2005), pp. 1597–1614 (cit. on pp. 2, 3).
- [YGJ08] Hyejin Youn, Michael T. Gastner, and Hawoong Jeong. “Price of Anarchy in Transportation Networks: Efficiency and Optimality Control”. In: *Physical Review Letters* 101 (Sept. 2008) (cit. on p. 1).
- [YP10] D. Yu and U. Parlitz. “Inferring local dynamics and connectivity of spatially extended systems with long-range links base on steady-state stabilization”. In: *Physical Review E*. 82 (Aug. 2010) (cit. on p. 4).
- [YTC02] M. Yeung, J. Tegnér, and J. Collins. “Reverse engineering gene networks using singular value decomposition and robust regression”. In: *Proceedings of the National Academy of Sciences USA* 99 (9 2002), pp. 6163–6168 (cit. on p. 4).

A Proofs for Section 3.2, Identifiability of the Diffusion

Lemma 5. Let $M = M^* + H$ be a diffusion matrix, such that for all $t \geq 0$, we have $S(t) \in \ker(H)$, $I(t) \in \ker(H)$ and $R(t) \in \ker(H)$. Let us check $(S, I, R) = \Phi(M^*)$ is then a solution of Equation (2) with diffusion matrix equal to M . Indeed, for all $t \geq 0$, we have

$$\begin{aligned} \frac{dS}{dt}(t) &= -\beta S(t) \odot I(t) + M^* S(t) \quad \text{by assumption} \\ &= -\beta S(t) \odot I(t) + M^* S(t) + HS(t) \quad \text{as } S(t) \in \ker H \\ &= -\beta S(t) \odot I(t) + MS(t). \end{aligned}$$

Likewise, I and R satisfy the corresponding equations, with diffusion matrix M instead of M^* . Now, (S, I, R) satisfies the differential equation Equation (2) with diffusion matrix M , and starts at the initial condition X_0 . Therefore, by unicity of the solutions of this system, we have $(S, I, R) = \Phi(M)$. \square

To prove Lemma 6, we first prove that the trajectories generated by a *linear* system often generate the whole space. Before doing this, we need the following technical lemmas.

Lemma 11 (Technical Result). *For every integer $N \geq 1$, let $(\lambda_n)_{1 \leq n \leq N}$ and $(t_k)_{1 \leq k \leq N}$ be two families of distinct (within each family) real numbers. Then, for every $\bar{N} \geq 1$, the following property holds true:*

$$\mathcal{P}(N) : \quad \forall 1 \leq n \leq N, \sum_{k=1}^N \mu_k e^{\lambda_n t_k} = 0 \Rightarrow (\forall 1 \leq k \leq N, \mu_k = 0).$$

Proof. We prove it by induction on N . The case $N = 1$ is immediate. Let $N \geq 2$, and let us show that if $\mathcal{P}(N-1)$ holds, then $\mathcal{P}(N)$ holds as well. Assume that for all $1 \leq n \leq N$, we have $\sum_{k=1}^N \mu_k e^{\lambda_n t_k} = 0$. Then, for all $1 \leq n \leq N$, we have

$$\sum_{k=1}^{N-1} \mu_k e^{\lambda_n (t_k - t_N)} + \mu_N = 0.$$

Let us consider the mapping:

$$g : \mathbb{R} \ni \lambda \mapsto \sum_{k=1}^{N-1} \mu_k e^{\lambda (t_k - t_N)} + \mu_N.$$

Then, g has N distinct roots (the λ_n 's), therefore by Rolle's theorem, its derivative admits $N-1$ distinct roots. We therefore obtain $N-1$ values λ'_n such that, for all $1 \leq n \leq N-1$, $\lambda_n < \lambda'_n < \lambda_{n+1}$ and $\frac{dg}{d\lambda}(\lambda'_n) = 0$. As a result, for all $1 \leq n \leq N-1$, we have

$$0 = \frac{dg}{d\lambda}(\lambda'_n) = \sum_{k=1}^{N-1} \mu_k (t_k - t_N) e^{\lambda'_n (t_k - t_N)}.$$

By induction, for all $1 \leq k \leq N-1$, we have $\mu_k (t_k - t_N) = 0$, and therefore $\mu_k = 0$, as the t_k 's are distinct. Then, $\mu_N = 0$ as well, hence the result. \square

We need the following lemma. Though well-known, we could not locate a reference, so added it here for completeness.

Lemma 12 (Almost Every Diffusion Matrices has Distinct Eigenvalues). *Almost every diffusion matrix has N distinct eigenvalues.*

Proof. Let \mathcal{E} be the subset of diffusion matrices which do not have N distinct eigenvalues, and let us prove it has null measure. We know that \mathcal{E} is the zero set of the discriminant Δ applied to the characteristic polynomial (Lang 2012), defined for every matrix A of order N by

$$F(A) = \Delta \circ \det(X \text{Id} - A).$$

The set of diffusion matrices is contained in the linear subspace of matrices A satisfying $1_N^T A = 0$, which is of dimension $N^2 - N$. We equip it with the standard Lebesgue measure over $\mathbb{R}^{N^2 - N}$.

Then, for any diffusion matrix $D \notin \mathcal{E}$, and any diffusion matrix M , $D + \lambda M$ is in \mathcal{E} only for a finite number of $\lambda \in \mathbb{R}$. Indeed, $\lambda \mapsto F(D + \lambda M) = \Delta \circ \det(X \text{Id} - D - \lambda M)$ is a polynomial function, so it is either zero or has a finite number of zeroes. But then it is nonzero at $\lambda = 0$, because $D \notin \mathcal{E}$. Therefore, the indicator function χ of \mathcal{E} is zero almost everywhere on $\{D + \lambda M, \lambda \in \mathbb{R}\}$, so it is also zero almost everywhere on $\{M + \lambda D, \lambda \in \mathbb{R}\}$.

Let us finally fix some $D \notin \mathcal{E}$, and some vector space \mathcal{H} such that $H \oplus \text{Vect}(D) = \{A, 1_N^T A = 0\}$. Thanks to the Fubini-Tonelli theorem, we have

$$\begin{aligned} \int_{\mathbb{R}^{N^2 - N}} \chi(A) dA &= \int_{\mathcal{H}} \int_{\mathbb{R}} \chi(A + \lambda D) d\lambda dA \\ &= \int_{\mathcal{H}} 0 = 0. \end{aligned}$$

Therefore, \mathcal{E} has zero Lebesgue measure. □

Lemma 13 (Almost Everywhere Identifiability, linear case). *Let $0 \leq t_1 < \dots < t_N < \infty$ be a subdivision of the nonnegative real half-axis, $M \in \mathcal{M}_N(\mathbb{R})$, and $y_0 \in \mathbb{R}^N$. Let y be the solution of the following differential equation:*

$$\begin{cases} \frac{dy}{dt} = My \\ y(0) = y_0. \end{cases} \quad (4)$$

Then, $(y(t_1), \dots, y(t_N))$ is a basis of \mathbb{R}^N for almost every M, y_0 .

Proof. Let us prove the result for M and y_0 satisfying the additional assumptions that all the eigenvalues of M have multiplicity 1, and that every coordinate of y_0 in an eigenbasis of M is nonzero (note that as M has N distinct eigenvalues, the associated subspaces are 1-dimensional, so the eigenbasis is unique up to permutation or scaling of the vectors). Thanks to Lemma 12, we will then have proved the result as stated, that is for almost every M , and also almost every y_0 (since the y_0 's with at least one 0 coordinate live in a union of N hyperplanes $x_i = 0$ where x_i is i -th the coordinate in the eigenbasis, which has zero Lebesgue measure.).

Since y satisfies the linear equation $dy/dt = My$, we know that, for all $t \geq 0$, we have $y(t) = \exp(tM)S_0$. Let us write $\lambda_1, \dots, \lambda_N$ the distinct eigenvalues of M , and (e_n) a corresponding eigenbasis. For all $t \geq 0$, we can decompose $y(t)$ along this eigenbasis. Let us write $y_1(t), \dots, y_N(t)$ the corresponding coefficients so that, for all $t \geq 0$, we have $S(t) = \sum_n y_n(t)e_n$. By assumption, for every n , we have $y_n(0) \neq 0$. As a result, for every $t \geq 0$, we have

$$\begin{aligned} y(t) &= \exp(Mt) y_0 = \exp(Mt) \sum_n y_n(0) e_n \\ &= \sum_n \exp(tM) y_n(0) e_n = \sum_n \exp(t\lambda_n) y_n(0) e_n. \end{aligned}$$

We want to show that $(y(t_k))_{1 \leq k \leq N}$ is a basis of \mathbb{R}^N . Let $\sum_k \mu_k y(t_k) = 0$ be a linear dependence relation. Since we have

$$\begin{aligned} \sum_{k=1}^N \mu_k y(t_k) &= \sum_{k=1}^N \mu_k \sum_n e^{t_k \lambda_n} y_n(0) e_n \\ &= \sum_n y_n(0) e_n \sum_{k=1}^N \mu_k e^{t_k \lambda_n}, \end{aligned}$$

we know that, for all $n \in \mathcal{N}$, we have

$$\sum_{k=1}^N \mu_k e^{t_k \lambda_n} = 0,$$

using the unicity of coordinates in the basis $(e_n)_n$ and the fact that for all node n , we have $y_n(0) \neq 0$. We use Lemma 11 to conclude. \square

We can now prove Lemma 6.

Proof. Let $K = S + I + R$ be the total population irrespective of infection status (for each node n , $K_n = S_n + I_n + R_n$ is the population of node n). By definition, for all $t \geq 0$, $K(t)$ is in the space generated by the trajectories. Then, K follows the differential equation

$$\begin{aligned} \frac{dK}{dt} &= \frac{dS}{dt} + \frac{dI}{dt} + \frac{dR}{dt} \\ &= -\beta S \odot I + MS + \beta S \odot I - \delta I + MI + \delta I + MR \\ &= MK. \end{aligned}$$

Using Lemma 13, we see that $(K(t_1), \dots, K(t_N))$ generates \mathbb{R}^N for almost every M , and $K(0) = S_0 + I_0 + R_0$, so for almost every M, S_0, I_0, R_0 . As a result, for almost every M , $X_0 = (S_0, I_0, R_0)$, the space generated by the trajectories contains a family which generate \mathbb{R}^N . This proves our claim. \square

B Proofs for 4.1, analysis of the influence of the diffusion rate

Let us first prove the following result.

Lemma 14 (Trajectories Close to a Line for Infinitely Quick Diffusion). *Let us assume the initial condition X_0 is such that S_0, I_0 and R_0 are proportional to the stationary distribution.*

For every $\tau > 0$, let us write Φ^τ the solution of the system of Equation (2) where M is replaced by M/τ , that is, for every $t \geq 0$, $\Phi_t^\tau = (S_\tau(t), I_\tau(t), R_\tau(t))$. Then, for all $T > 0$,

$$\sup_{0 \leq t \leq T} d(S_\tau(t), \mathbb{R}\tilde{\mu}_M) \rightarrow 0,$$

when $\tau \rightarrow \infty$, and likewise for I_τ and R_τ .

The results extends to cases when X_0 is not proportional to the stationary distribution, only taking the supremum over some interval $[t(\tau), T]$, where $t(\tau)$ tends to 0, when $\tau \rightarrow 0$, and $t(\tau)$ represents the time it takes for the system to converge to the stationary distribution.

Proof. First, for all $\tau > 0$, and $t \geq 0$, we have

$$S_\tau(t) = \left(\sum_n S_{\tau,n}(t) \right) \tilde{\mu}_M + \nu_\tau(t), \quad (5)$$

where $\nu_\tau(t)$ belongs to the set $\mathcal{H} = \{\nu \in \mathbb{R}^N \mid \sum_n \nu_n = 0\}$ ⁶. Moreover, $\nu_\tau(t)$ is bounded uniformly in $\tau > 0$ and $t \geq 0$, as all the $S_\tau(t)$'s are bounded by the total population, that is the sum of the coordinates of the initial condition X_0 .

Then, for all $\tau > 0$, $t \mapsto \nu_\tau(t)$ is differentiable thanks to Equation (5) and, by differentiating Equation (5), we see ν_τ satisfies a differential equation of the form:

$$\frac{d\nu_\tau}{dt}(t) = \frac{M}{\tau} \nu_\tau(t) + \gamma_\tau(t),$$

where γ_τ is a quantity depending on many things, but which is uniformly bounded in $\tau > 0$ and $t \geq 0$, again thanks to the fact that the $S_\tau(t)$'s, the $I_\tau(t)$'s and the $R_\tau(t)$'s are bounded by the total size of the population. Moreover, for all $\nu \in \mathbb{R}^N$, we have $M\nu \in \mathcal{H}$, since the columns of M sum to 0. As a result, for all $\tau > 0$, and all $t \geq 0$, we have $\frac{d\nu_\tau}{dt}(t) \in \mathcal{H}$ (since \mathcal{H} is a finite dimensional vector space, so derivatives of functions living on it stay in it), and $\frac{M}{\tau} \nu_\tau(t) \in \mathcal{H}$ (by what precedes), so that $\gamma_\tau(t)$ also belongs to \mathcal{H} .

Finally, for all $\tau > 0$, and all $t \geq 0$, we have

$$\begin{aligned} \nu_\tau(t) &= \exp\left(\frac{M}{\tau}t\right) \nu_\tau(0) + \int_0^t \exp\left(\frac{M}{\tau}(t-s)\right) \gamma_\tau(s) ds \\ &= \int_0^t \exp\left(\frac{M}{\tau}(t-s)\right) \gamma_\tau(s) ds, \end{aligned}$$

since $\nu_\tau(0) = 0$, as the initial condition is proportional to $\tilde{\mu}_M$ by assumption. Let us now fix $\varepsilon > 0$. Let $B \subset \mathcal{H}$ be a ball such that that, for all $\tau > 0$ and $t \geq 0$, we have $\gamma_\tau(t) \in B$. Since M only has eigenvalues with (strictly) negative eigenvalues on \mathcal{H} , we may find some threshold $u_{\min} > 0$ such that, for all $u \geq u_{\min}$, for all $\nu \in B$, we have

$$\|\exp(Mu)\nu\| < \varepsilon.$$

Moreover, there exists a constant $\kappa \geq 1$ such that, for all $u \geq 0$, for all $\nu \in B$, we have $\|\exp(Mu)\nu\| \leq \kappa$. Let us now consider $\tau \leq \frac{1}{u_{\min}} \frac{\kappa}{\varepsilon}$ (it is chosen so that, for $t-s \geq \frac{\varepsilon}{\kappa}$, we have $\frac{t-s}{\tau} \geq u_{\min}$). Therefore, for all $t \leq T$, we have

$$\begin{aligned} \|\nu_\tau(t)\| &\leq \int_0^t \left\| \exp\left(\frac{M}{\tau}(t-s)\right) \gamma_\tau(s) \right\| ds \\ &= \int_0^{\frac{\varepsilon}{\kappa}} \left\| \exp\left(\frac{M}{\tau}(t-s)\right) \gamma_\tau(s) \right\| ds \\ &\quad + \int_{\frac{\varepsilon}{\kappa}}^T \left\| \exp\left(\frac{M}{\tau}(t-s)\right) \gamma_\tau(s) \right\| ds \\ &\leq \frac{\varepsilon}{\kappa} + \int_{\frac{\varepsilon}{\kappa}}^T \varepsilon ds \\ &\leq \varepsilon + \varepsilon \left(T - \frac{\varepsilon}{\kappa}\right) \leq \varepsilon(1+T). \end{aligned}$$

As a result, for all $\tau \leq \frac{1}{u_{\min}} \frac{\kappa}{\varepsilon}$, with u_{\min} and κ chosen independently of τ , we have $\sup_{0 \leq t \leq T} \|\nu_\tau(t)\| \leq \varepsilon(1+T)$. We have therefore proven that $d(S_\tau(t), \mathbb{R}\tilde{\mu}_M) \rightarrow 0$, as $\tau \rightarrow 0$. We would prove likewise the result for I_τ and R_τ , which concludes the proof. \square

⁶This is a consequence of the decomposition $\mathbb{R}^N = \mathbb{R}\tilde{\mu}_M \oplus \mathcal{H}$.

We can now prove Lemma 7.

Proof. Let $T > 0$. Now, let us write, for all $t \geq 0$, using the notations of the proof of Lemma 14,

$$S^\tau(t) = s_\tau(t)\tilde{\mu}_M + \nu_\tau(t), \quad (6)$$

and likewise for I^τ and R^τ . Since S_0, I_0 and R_0 are proportional to the stationary distribution, we know, thanks to Lemma 14, that $\nu^\tau(t)$ tends towards 0, uniformly on each $[0, T]$, with $T \geq 0$. Since for all τ , S^τ, I^τ and R^τ are nonnegative, and bounded by the total population, the family of functions (s^τ, i^τ, r^τ) , defined on $[0, T]$, has values in a bounded set of the continuous functions from \mathbb{R}_+ to \mathbb{R}^3 , endowed with the infinity norm on each of s, i and r , that is $\|(s, i, r)\|_\infty = \max(\|s\|_\infty, \|i\|_\infty, \|r\|_\infty)$. Moreover since, for all $\tau \geq 0$, for all $0 \leq t \leq T$, we have

$$S^\tau(t) = S^\tau(0) - \int_0^t \beta S^\tau(s) \odot I^\tau(s) + \frac{M}{\tau} S^\tau(s) ds,$$

we obtain, summing along the coordinates,

$$s^\tau(t) = s^\tau(0) - \sum_n \beta_n \tilde{\mu}_M(n)^2 \int_0^t s^\tau(s) i^\tau(s) ds.$$

As a result, s^τ is differential on $[0, T]$, its derivative satisfies

$$\frac{ds^\tau}{dt} = - \left(\sum_n \beta_n \tilde{\mu}_M(n)^2 \right) s^\tau(t) i^\tau(t),$$

and its derivative is therefore bounded on $[0, T]$, uniformly on τ . The same holds for i^τ and r^τ . Therefore, (s^τ, i^τ, r^τ) is equi-continuous. As a result, the family $((s^\tau, i^\tau, r^\tau))_{\tau \geq 0}$ is pre-compact (Sutherland 2004) in the Banach space of functions from $[0, T]$ to \mathbb{R}^3 , endowed with the infinity norm defined above, so that, provided it admits an unique adherence value, it converges towards this one.

Let us consider a converging subsequence, and still index it by τ , to simplify notations. As a result, the limit s satisfies

$$s(t) = s(0) + \sum_n \beta_n \tilde{\mu}_M(n)^2 \int_0^t s(s) i(s) ds,$$

and likewise for i and s . Moreover, for all $t \geq 0$, we know that $s^\tau(0) = \sum_n S^\tau(0) = \sum_n S_n(0)$ which does not depend on τ , therefore $s(0) = \sum_n S_n(0)$, and likewise for i_0 and r_0 . Therefore, (s, i, r) is solution of the scalar system described in the statement of the Lemma, and by uniqueness of the solutions of this system, satisfying the initial condition (s_0, i_0, r_0) , the tuple is uniquely defined. Therefore, the family of (s^τ, i^τ, r^τ) 's admits a unique adherence value, and converges towards this one. Plugging back into Equation (6), we see that $S^\tau \rightarrow s\tilde{\mu}_M$, as $\tau \rightarrow 0$, uniformly on $[0, T]$, and likewise for I^τ and R^τ , which concludes the proof. \square

Let us prove Corollary 8.

Proof. Applying the results of Lemma 7 with $T = t_K$, we know that the observation matrix writes

$$\begin{aligned} \hat{O}((t_k), \Phi^\tau(M)) = \\ \tilde{\mu}_M \otimes (s(t_1), \dots, s(t_K), i(t_1), \dots, i(t_K), r(t_1) \dots r(t_K)) \\ + O(\varepsilon(\tau)), \quad (7) \end{aligned}$$

as $\tau \rightarrow 0$, where $\varepsilon(\tau) \rightarrow 0$, when $\tau \rightarrow 0$. Indeed, using the notations of the proof of Lemma 7, we know that for each $1 \leq k \leq K$, the column $S(t_k)$ of the observation

matrix (for instance), writes $S(t_k) = s(t_k)\bar{\mu}_M + \nu_\tau(t_k)$, and ν_τ tends to 0, as $\tau \rightarrow 0$, uniformly on $[0, t_K]$. The first term of Equation (7) is of rank 1, as $s + i + r = 1$, identically. The conclusion follows from the continuity of the numerical rank of a matrix (the numerical rank is the number of singular values greater than some threshold, and these values depend continuously on the matrix). \square

C Proofs for Section 5.1, symmetries

Let us first show the effect of node-renumbering on the trajectories.

Lemma 15 (Node re-numbering). *Let $\mathcal{M} = (M, (\beta, \delta), X_0)$ be a model and P a permutation matrix. Then, for all $t \geq 0$, we have*

$$\begin{aligned}\Phi_t(P \cdot \mathcal{M}) &= P \cdot \Phi_t(\mathcal{M}) \\ &= (PS(t), PI(t), PR(t)),\end{aligned}$$

writing $(S(t), I(t), R(t)) = \Phi_t(\mathcal{M})$, and using the conventions of Section 2.4.

This implies immediately that if P is the matrix of an automorphism of our model, then for all $t \geq 0$, we have $\Phi_t(P \cdot \mathcal{M}) = \Phi_t(\mathcal{M})$, and therefore $P \cdot \Phi_t(\mathcal{M}) = \Phi_t(\mathcal{M})$. In other words, if i and j are in a same orbit of P , then the trajectories at nodes i and j are the same: for all $t \geq 0$, $S_i(t) = S_j(t)$, and likewise for I and R .

Proof. Let us show that (PS, PI, PR) is a solution of the differential equation also satisfied by the flow $\Phi(PMP^{-1}, (P\beta, P\delta), PX_0)$, which is enough to conclude by unicity of the solutions sharing the same initial condition. Let $1 \leq i \leq N$. Then, we have

$$\begin{aligned}\frac{d}{dt}[PS]_i &= \left[P \frac{dS}{dt} \right]_i \\ &= \frac{dS_{\sigma(i)}}{dt} \\ &= -\beta_{\sigma(i)} S_{\sigma(i)} I_{\sigma(i)} + [MS]_{\sigma(i)} \\ &= -[P\beta]_i [PS]_i [PI]_i + [PMS]_i \\ &= -[P\beta]_i [PS]_i [PI]_i + [(PMP^{-1})(PS)]_i.\end{aligned}$$

Therefore, we have

$$\frac{dPS}{dt} = -(P\beta) ((PS) \odot (PI)) + (PMP^{-1})(PS).$$

So PS satisfies the required equation, and I, R do as well, which we show using the same method, and which allows us to conclude. \square

We can now prove Lemma 9.

Proof. Let us first prove 3) \Rightarrow 2). Let $\sigma \in \mathcal{H}$. For any $x \in \mathcal{H}$, we have

$$\begin{aligned}P(\sigma)MP(\sigma)^{-1}x &= P(\sigma)Mx \quad \text{as } x \in \text{Fix}(\mathcal{H}) \\ &= Mx \quad \text{as } Mx \in \text{Fix}(\mathcal{H}).\end{aligned}$$

We now average the nodes which give the same trajectories, which is the standard method of averaging under a group action. Let

$$\bar{M} = \frac{1}{\#\mathcal{H}} \sum_{\sigma \in \mathcal{H}} P(\sigma)MP(\sigma)^{-1}.$$

We therefore obtain by construction that, for all $X_0 \in \text{Fix}(\mathcal{H})$, we have $\mathcal{H} \subset \text{Aut}(\bar{M}, (\beta, \delta), X_0)$. The fact \bar{M} and M agree on $\text{Fix}(\mathcal{H})$ is a direct consequence of

the averaging. Now, since \bar{M} is symmetric with respect to \mathcal{H} , thanks to Lemma 15, we know that the trajectories it generates are also symmetric with respect to \mathcal{H} . As a result, they belong to $\text{Fix}(\mathcal{H})$. Therefore, they also satisfy the differential equation with M , as we have just proven that M and \bar{M} agree on $\text{Fix}(\mathcal{H})$.

Then, 2) \Rightarrow 1) is a direct consequence of Lemma 15.

To prove 1) \Rightarrow 3), let $S_0 \in \text{Fix}(\mathcal{H})$, and let us show that $MS_0 \in \text{Fix}(\mathcal{H})$. Choose I_0 and R_0 such that $I_0 \in \text{Fix}(\mathcal{H})$, and define $X_0 = (S_0, I_0, R_0)$. For every $\sigma \in \mathcal{H}$, for every node i , we have

$$[MS(0)]_{\sigma(i)} = \frac{dS_{\sigma(i)}}{dt}(0) + \beta_{\sigma(i)}S_{\sigma(i)}(0)I_{\sigma(i)}(0).$$

Now, $\beta_{\sigma(i)} = \beta_i$ by assumption on the coefficients, and $S_{\sigma(i)}(0)I_{\sigma(i)}(0) = S_i(0)I_i(0)$ by assumption. Moreover, we have

$$\begin{aligned} \frac{dS_{\sigma(i)}}{dt}(0) &= \lim_{t \rightarrow 0} \frac{S_{\sigma(i)}(t) - S_{\sigma(i)}(0)}{t} = \lim_{t \rightarrow 0} \frac{S_i(t) - S_i(0)}{t} \\ &= \frac{dS_i}{dt}(0), \end{aligned}$$

where the second equality is a consequence of the fact that trajectories remain in $\text{Fix}(\mathcal{H})$. As a result, we have

$$[MS(0)]_{\sigma(i)} = \frac{dS_i}{dt}(0) + \beta_i S_i(0)I_i(0) = [MS(0)]_i.$$

Therefore, for every $\sigma \in \mathcal{H}$, we have $P(\sigma)MS_0 = MS_0$ so that, by definition, we have $MS_0 \in \text{Fix}(\mathcal{H})$. □

Corollary 10. Let us first prove that $Z = M - \bar{M}$ vanishes on $\text{Fix}(\mathcal{H})$. For all $X_0 \in \text{Fix}(\mathcal{H})$, since M and \bar{M} produce the same trajectories, we have, for all $t \geq 0$,

$$\frac{dS}{dt} = -\beta S(t) \odot I(t) + MS(t) = -\beta S(t) \odot I(t) + M'S(t),$$

so that $ZS(t) = (M - M')S(t) = 0$. As a result, $ZS(0) = 0$. This is true for all $S(0) \in \text{Fix}(\mathcal{H})$ (as $X_0 = (S_0, I_0, R_0)$ is arbitrary provided S_0, I_0 and R_0 all belong to $\text{Fix}(\mathcal{H})$), so Z vanishes on $\text{Fix}(\mathcal{H})$. □

Corollary 10. This result is a particular case of the following Lemma 16, when we let \mathcal{H} be the set of permutations under which the trajectories are invariant. In that case, the number of orbits of \mathcal{H} is the number of different trajectories. □

Lemma 16 (Matrices vanishing on $\text{Fix}(\mathcal{H})$). *For any group of permutations \mathcal{H} , a basis of the space of matrices Z vanishing on $\text{Fix}(\mathcal{H})$ is given by the $Z^{i,j,k}$'s introduced before Corollary 10, where i and j are in the same orbit under \mathcal{H} . Consequently, the dimension of this space is*

$$(N - 1)\#\{\text{orbits under } \mathcal{H}\}.$$

Proof. Let Z be such a matrix. As $Z = M - M'$ with M, M' diffusion matrices, the columns of Z have vanishing sums. Moreover, Z has to vanish on any vector fixed by \mathcal{H} . These vectors are precisely the $x \in \mathbb{R}^N$ such that $x_i = x_{\sigma(i)}$ for all $i \in \mathcal{N}$, and for all $\sigma \in \mathcal{H}$. Thus, they are the x 's such that $E_{k,i}x = E_{k,\sigma(i)}x$ for every $i, k \in \mathcal{N}$, and $\sigma \in \mathcal{H}$. Therefore, $Z^{i,j,k}x = 0$ for all $x \in \text{Fix}(\mathcal{H})$ when i, j, k satisfy

the assumptions of the lemma. The $Z^{i,j,k}$'s are clearly linearly independent. Let us show that they generate the space of all Z 's.

Let Z vanish on $Fix(\mathcal{H})$. We will make all of the coefficients of Z vanish by subtracting multiples of $Z^{i,j,k}$ s, which will prove that Z is indeed a linear combination of the $Z^{i,j,k}$ s. Let $\mathcal{O} = \{i_1 < \dots < i_m\}$ be an orbit of $\{1, \dots, n\}$ of cardinal m under the action of \mathcal{H} .

Let us remark that for $1 \leq k \leq N-1$, $1 \leq l < m$, $Z^{i_l, i_{l+1}, k}$ satisfies the conditions of the lemma and has its (k, i_l) coefficient equal to 1, its (k, i_{l+1}) coefficient equal to -1.

Therefore, $Z - Z_{k, i_1} Z^{i_1, i_2, k}$ has its (k, i_1) coefficient equaling zero, and its (k, i_2) coefficient equal to $Z_{k, i_2} + Z_{k, i_1}$, and aside from the last line (which we will ignore for the moment) these are the only coefficients changing.

Then, if $m \geq 3$, we can reiterate this by considering $Z - Z_{k, i_1} Z^{i_1, i_2, k} - (Z_{k, i_2} + Z_{i_1, k}) Z^{i_2, i_3, k}$ and the obtained matrix will have the (k, i_2) coefficient vanishing and the (k, i_3) coefficient changing to $Z_{k, i_3} + Z_{k, i_2} + Z_{k, i_1}$, and the (k, i_1) coefficient is still 0.

We iterate this method exactly $m-1$ times to obtain Z' . By construction, Z' has each of the (k, i_l) , $1 \leq l \leq m$ coefficients vanishing except maybe the $l = m$ one, equaling $Z_{k, i_1} + \dots + Z_{k, i_m}$.

But then this one is also zero. Indeed, if $(e_j)_j$ is the canonical basis, as $\sum_{l=1}^m e_{i_l} \in Fix(H)$, we have $Z' \sum_{l=1}^m e_{i_l} = 0$, and by looking the k -th coefficient, we obtain $Z'_{k, i_m} = Z_{k, i_1} + \dots + Z_{k, i_m} = 0$.

We can then iterate this construction on every line except the last (meaning for $1 \leq k \leq N-1$) and every orbit to obtain Z'' . By construction, every line of Z'' is zero, except maybe the last ($k = N$), but then as the columns of Z'' have a vanishing sum (as Z'' is a linear combination of Z and the $Z^{i,j,k}$), $Z'' = 0$. Thus, Z is in the space generated by the $Z^{i,j,k}$.

□